Quaternary Sediment Sources to Hemipelagic and Contourite Depositional Settings off the Iberian Margin, IODP Sites 1385 and 1391

Senior Thesis

Submitted in partial fulfillment of the requirements for the

Bachelor of Science Degree

At The Ohio State University

By

John Daniele

The Ohio State University

2016

Approved by

Larry Krissek, Advisor
School of Earth Sciences

Table of Contents

Abstract

Expedition 339 of the Integrated Ocean Drilling Program (IODP), located on the western Iberian Margin and the Gulf of Cadiz, gathered sediment cores in order to investigate the Mediterranean Outflow Water (MOW) and its paleoceanographic significance on the North Atlantic Ocean climate and circulation history. The rapid sedimentation rate from the MOW allows for a detailed look at the sedimentary record. Aboard the JOIDES Resolution, sediment cores were collected at Sites U1385 and U1391 and analyzed by using the X-diffraction (XRD) method to determine their bulk mineralogy. In this study, the shipboard data were processed using Paleontological Statistics (PAST) software for principal component analysis. This analysis identified covariations among minerals, thereby defining mineral assemblages that could be used to determine sediment origin. At Site U1385, the three most important principal components defined four mineral assemblages that included chlorite, plagioclase, K-feldspar and augite. At Site U1391, the three most important principal components defined five mineral assemblages consisting of chlorite, K-feldspar, plagioclase, augite and aragonite. No definite correlation to the provenance could be made, but the mineral assemblages defined by principal component analysis are hypothesized to be the result of changes in grain size. The abundance of chlorite indicates the presence of smaller grain sizes carried by weaker currents, while plagioclase, K-feldspar and augite indicate silicic to intermediate continental source rocks and larger grains transported by stronger currents. The differences in associations of plagioclase and K-feldspar

at Sites U1385 and U1391 suggest some differences in the sediment sources to these two sites.

Acknowledgements

First, I would like to thank Dr. Larry Krissek for serving as my thesis advisor on such short notice. His guidance, patience, and understanding helped me tremendously throughout this challenging process. Thank you for allowing me the opportunity to learn and work with you as both my professor and advisor. I would also like to thank Dr. Anne Carey for helping me with the thesis writing and for all her advice and guidance during my college career.

Second, I would like to thank all my Earth science professors and classmates who were a part of my undergraduate journey, especially Ryan Haugh and Christina Jauregui for pushing me through the finish line. Their support, friendship, and knowledge gave me the motivation I needed to continue moving forward in pursuit of my degree in Earth science. I learned so much from every one of them and will forever cherish the time we had together.

Finally, I would like to give a special thanks to my parents, my aunt Laura, my brother Nick, my sister Gina, and my girlfriend Leonor. Their love, support, and encouragement gave me the strength I needed during the most challenging moments. They were always there for me when I needed them most and I am very grateful for everything they have done and continue to do for me. If it were not for my family, friends, and loved ones, I would not be where I am today.

Introduction

The Mediterranean Outflow Water (MOW) is a strong, warm, saline bottom current system that flows outward from the Mediterranean Sea to the north along the middle slope of the west Iberian Peninsula, due to the Coriolis effect and margin bathymetry. These bottom currents follow the contours of the margin, depositing material called contourites along their flow path. Contourites normally occur at a location with high sedimentation rates called a contourite deposition system (CDS), which are known to be very complex (Expedition 339 Scientists, 2013a).

The primary objective of Expedition 339 of the Integrated Ocean Drilling Program (IODP) was to collect and study sediment cores from various sites to determine the history of MOW and how MOW has affected circulation and climate of the North Atlantic Ocean. The data collected from this expedition allowed the scientists aboard to study and interpret climatic, paleoceanographic, and sea level changes from the Messinian to the present. The connections of these records proved the significance of ocean gateways in regional and global climate change and ocean circulation (Hernandez-Molina et al., 2013; Expedition 339 Scientists, 2013a).

During IODP Expedition 339, seven sites were drilled, with five sites in the Gulf of Cadiz and two sites off the West Iberian margin. Included in those seven sites were Sites U1385 and U1391, which were examined in this study. Six sites (U1386-U1391) were targeted in order to investigate the CDS (Figure 1) produced by the MOW influences and its evolution and environmental

implications. Not only does this CDS produce high rates of sediment accumulation on the Gulf of Cadiz and the West Iberian margin, but also it is a direct result of MOW. The sedimentary record found at these locations permits scientists to link paleocirculation patterns to past environmental changes (Expedition 339 Scientists, 2013a).

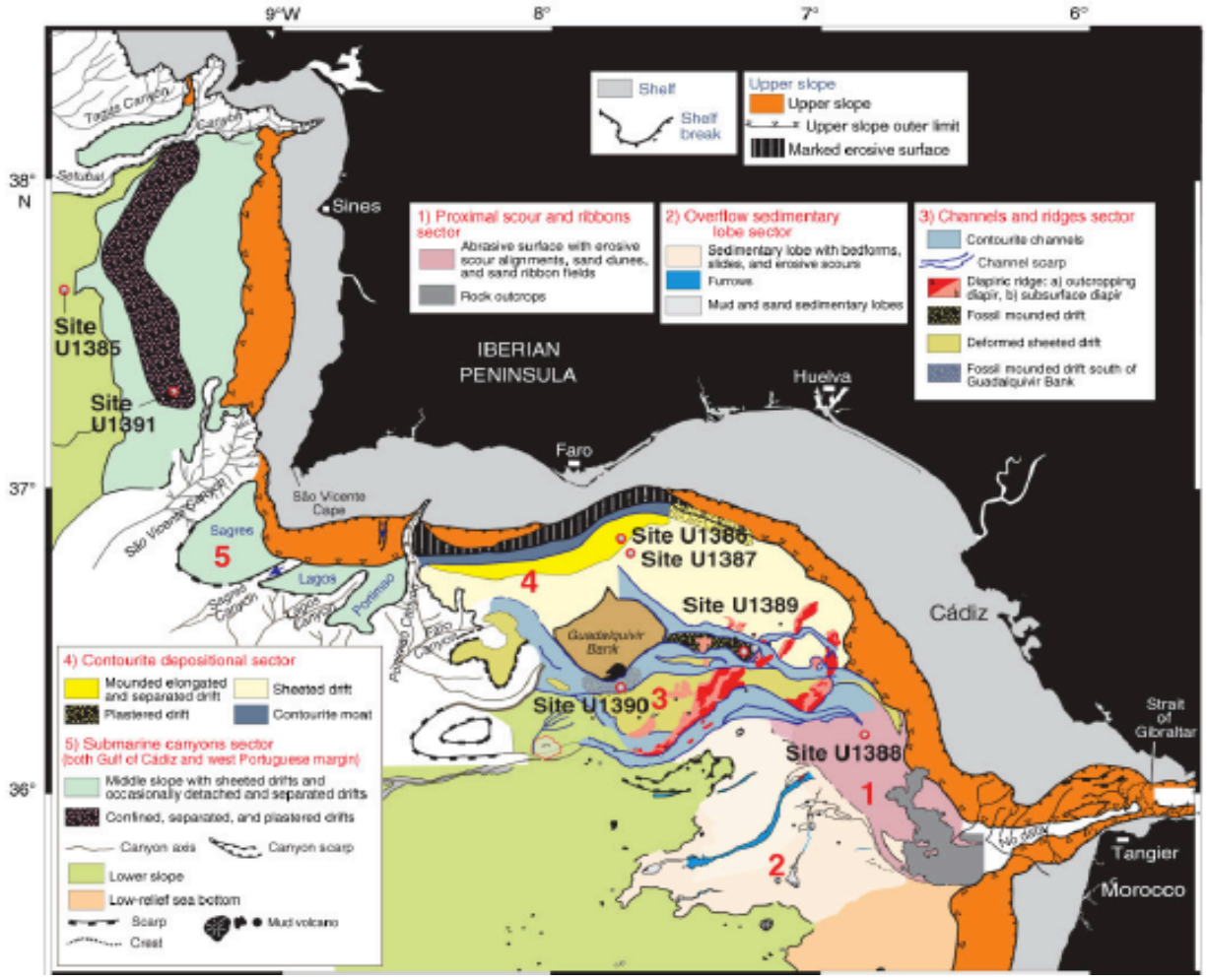

Figure 1: Contourite depositional system (CDS) and Expedition 339 site locations (Hernandez-Molina et al., 2013).

Site U1385 was drilled on the southwest Iberian margin at the so-called Shackleton site (Figure 2) in order to produce a marine reference section of Pleistocene millennial-scale climate variability and fluctuations in surface and deep-water circulation. This site is located on the deeper Portuguese margin sediments that are outside the influence of MOW and are, instead, dominated by hemipelagic muds with some variable mixtures of biogenic components and terrigenous sand and silt. During interglacial periods, pelagic sedimentation increased at Site U1385, whereas during glacial periods sediments included increased terrigenous material resulting from lowered sea level, increased concentration of turbidity currents, more ice rafting and more bottom currents. This site was positioned farther offshore in order to analyze relatively open-water conditions; at this site, some terrigenous sediment might have been supplied as wind-derived material from the Sahara Desert. (Expedition 339 Scientists, 2013a).

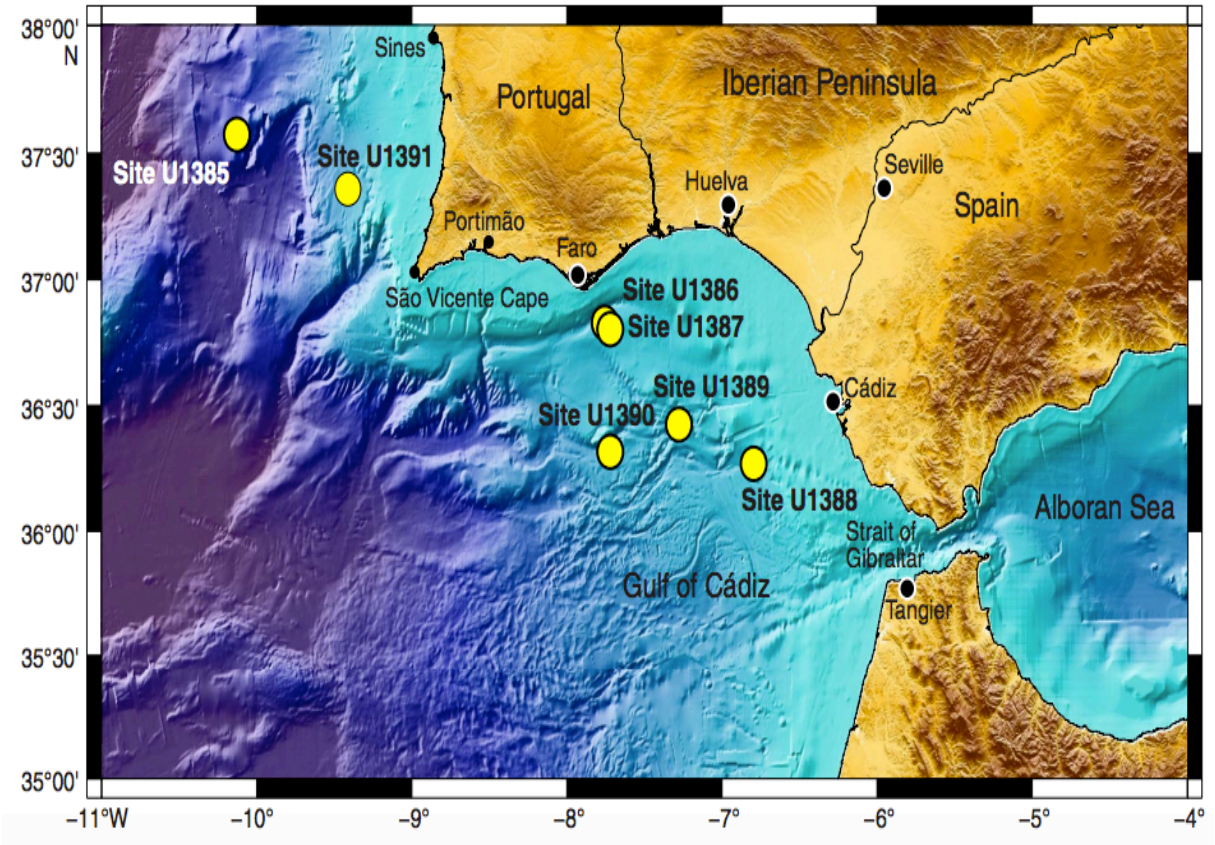

Figure 2: Expedition 339 site locations in the Gulf of Cadiz and West Iberian margin (Expedition 339 Scientists, 2013a).

Site U1391 was drilled on the southwest Iberian margin approximately 50 km northwest of the Portuguese city of Cape Sao Vicente (Figure 2). This site is situated over a large plastered drift stretching along the middle slope between Cape Sao Vicente and Setubal submarine canyons. Site U1391 is the most distal of the sites influenced by MOW that were drilled and, according to the Expedition 339 scientists, the extensive plastered drift at this location is considered a part of the Cadiz CDS. The deposits show a well-layered internal structure with laterally extensive aggradational units and some thickening towards the axial area of the drift. The sediments at Site U1391 are expected to

have been transported primarily along the margin by the MOW to this location (Expedition 339 Scientists, 2013a).

The difference in terrigenous sediment supply mechanisms for these two sites—predominantly along-slope at Site U1391, as compared to downslope/offshore +/- wind transport at Site U1385—suggests that the terrigenous sediments of these two sites were derived from different sources. As a result, it is reasonable to predict that the terrigenous sediments at these two sites should exhibit compositional differences. The goal of this study is to test that hypothesis, using shipboard mineralogical data and principal component analysis.

METHODS

X-ray diffraction (XRD) analyses were performed onboard the JOIDES Resolution during Expedition 339 using a Bruker D-4 Endeavor diffractometer fixed with a Vantec-1 detector and using nickel-filtered CuKα radiation. The machine voltage was 37 kV, with a current of 40 mA. At Site U1385 and Site U1391, a total of 16 samples and 37 samples were analyzed, respectively. One 5 cubic centimeter sample was taken approximately for every 10 meters downcore, was freeze-dried, and was ground in an agate ball mill or by hand. Bulk samples were mounted as pressed powders for XRD analyses. The samples were scanned over a range of 4°-70°2θ, with a step size of 0.0174°2θ, a divergence slit of 0.3mm, and a scan speed of 1 s/step (Expedition 339 Scientists, 2013b).

The XRD analysis identified only the most common mineral components and their relative abundances, whereas the EVA software package was utilized for mineral identification from the bulk diffractogram of a sample and its peak characteristics. Peak intensities for each mineral identified were documented to demonstrate how each mineral varied between their respective sites and downhole (Expedition 339 Scientists, 2013b).

In order to calibrate bulk XRD intensities, peak intensities for carbonate minerals were compared to independent measurements of carbonate content, as measured by coulometer. This only directly provides calibration of the XRD data to the abundance of carbonate minerals. However, the resultant data exhibited a good correlation between the amount of a mineral in a sediment

sample and the intensity of its diagnostic XRD peak (Expedition 339 Scientists, 2013b).

For this study, principal component analysis was used because it is a widely used statistical approach to determine relationships or lack of relationships between variables within a large data set. The data analysis was accomplished through the use of PAST software, version 3.11, which was downloaded from http://folk.uio.no/ohammer/past/. The shipboard XRD peak intensities for Sites U1385 and U1391 were copied and pasted from the IODP website into Excel files, which were then copied and pasted into the PAST software. The Site U1385 data file can be found at http://publications.iodp.org/proceedings/339/103/103_t6.htm, and the Site U1391 data file can be found at http://publications.iodp.org/proceedings/339/109/109_t3.htm. Before operating the PAST software, the data listed as "NA" in the Excel files were replaced with zeroes and the "core section" through column "339-" were deleted. Next, the "Row" box in PAST was unchecked, leaving the "Column" box checked. Then the rows and columns from "Quartz" through "Aragonite" were copied and pasted into the "name" row of the PAST software. The rows and columns from "Quartz" through "Aragonite" were then selected for principal component analysis. Finally, clicking on "Multivariate", "Ordination" and "Principal Components (PCA)" in that order ran the data analysis within PAST.

RESULTS

The principal component analysis for Site U1385 defines12 factors that explain 100% of the original data variance (Table 1). However, only the first three principal components are considered important, based on the amount of data variance described by each (Figure 3). These three factors explain approximately 77% of the total data variance (Figure 3). Principal Component 1 (Figure 4) accounts for approximately 38% of the variance and is defined by a high positive loading for plagioclase and a moderate negative loading for augite. Principal Component 2 (Figure 5) accounts for approximately 23% of the total variance and is defined by a high positive loading for chlorite. There is no comparable high negative loading in Principal Component 2. Principal Component 3 (Figure 6) accounts for approximately 16% of the total variance and is defined by high positive loadings for K-feldspar, plagioclase and augite. Pyrite, chlorite and dolomite have low negative loadings, much less than the magnitudes for K-feldspar, plagioclase and augite so the inverse relationship is relatively weak. Therefore, Principal Component 3 can be interpreted as mostly the indicating the presence/absence of covarying K-feldspar, plagioclase and augite. It is important to note, however, that pyrite will be ignored in the discussion of mineral assemblages because pyrite is a diagenetic mineral, rather than a detrital one. Table 2 shows the loading data for all 12 principal components at Site U1385, and Figure 3 shows the SCREE plot, which is a graphical representation of the eigenvalues in the Summary Data (Table 1).

Table 1: Site U1385 Data Summary

PC	Eigenvalue	% Variance
1	2.21E+05	3.81E+01
2	1.36E+05	2.34E+01
3	9.51E+04	1.64E+01
4	4.99E+04	8.60E+00
5	4.03E+04	6.95E+00
6	1.78E+04	3.06E+00
7	1.08E+04	1.86E+00
8	8.57E+03	1.48E+00
9	1.16E+03	2.00E-01
10	3.57E+00	6.15E-04
11	7.86E-01	1.35E-04
12	1.46E-01	2.51E-05

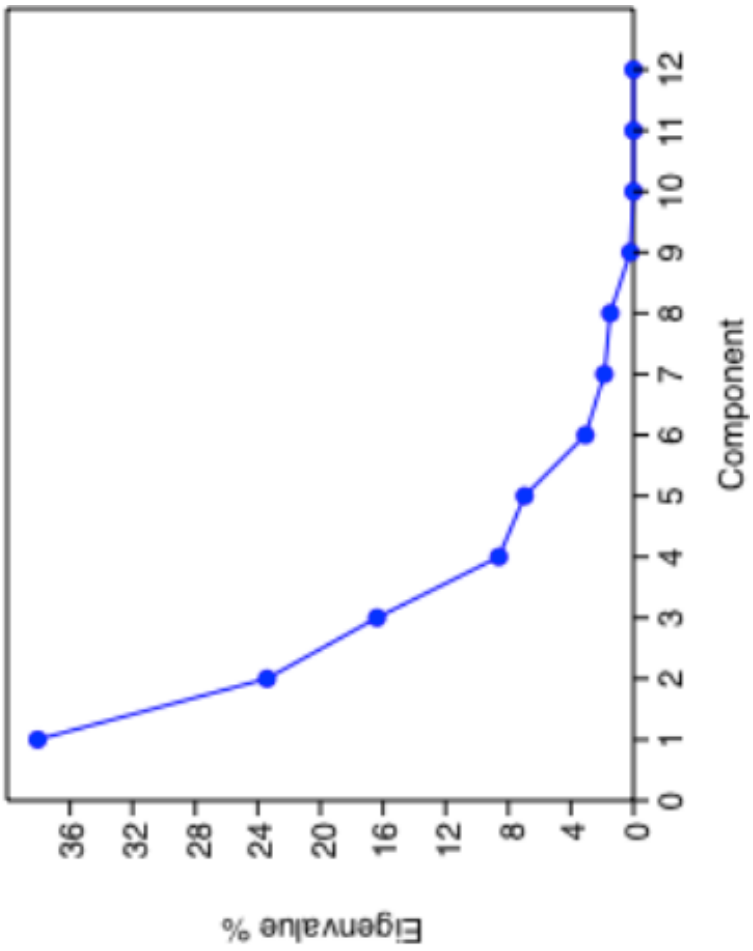

Figure 3: Site U1385 SCREE Plot

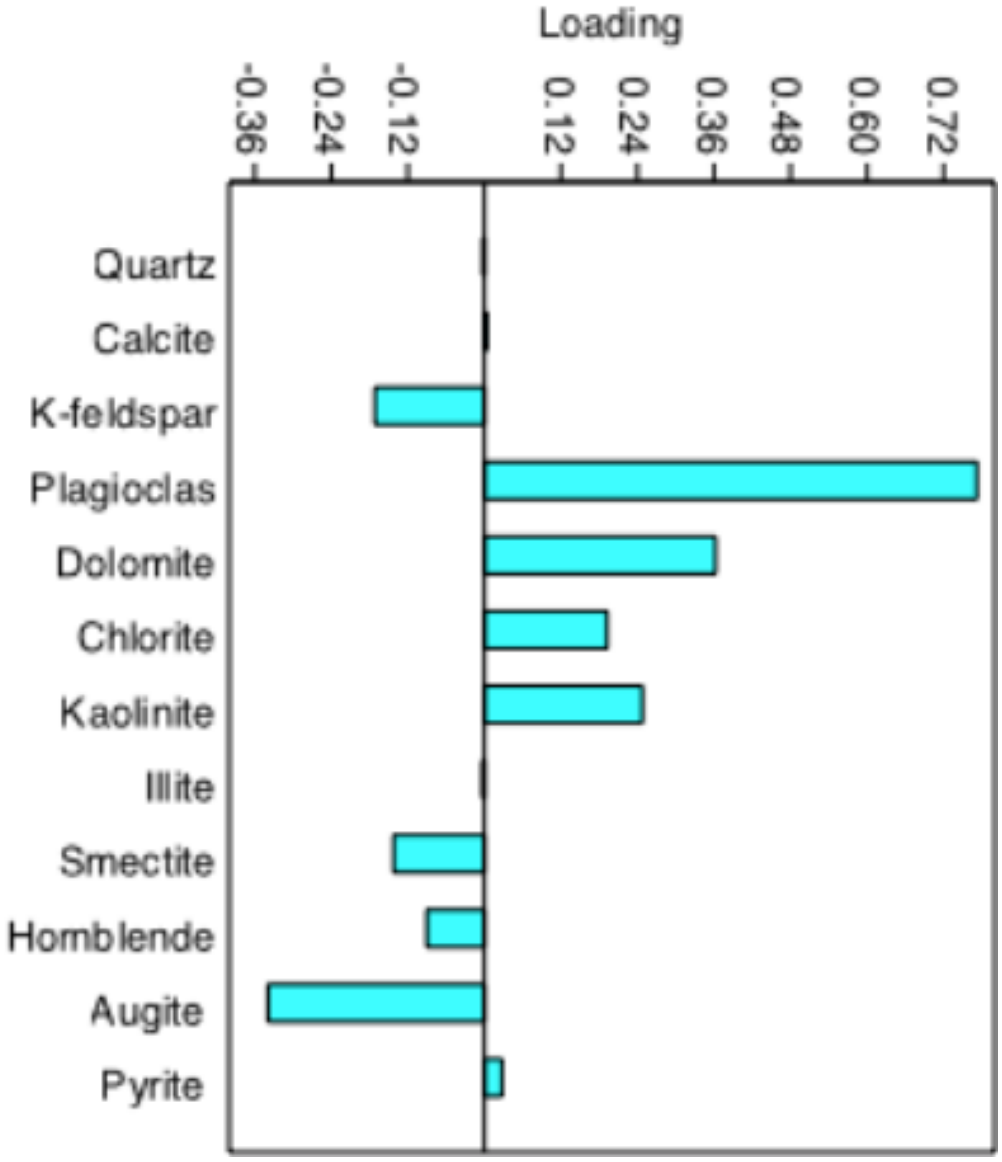

Figure 4: Site U1385 Loading Plot for Principal Component One

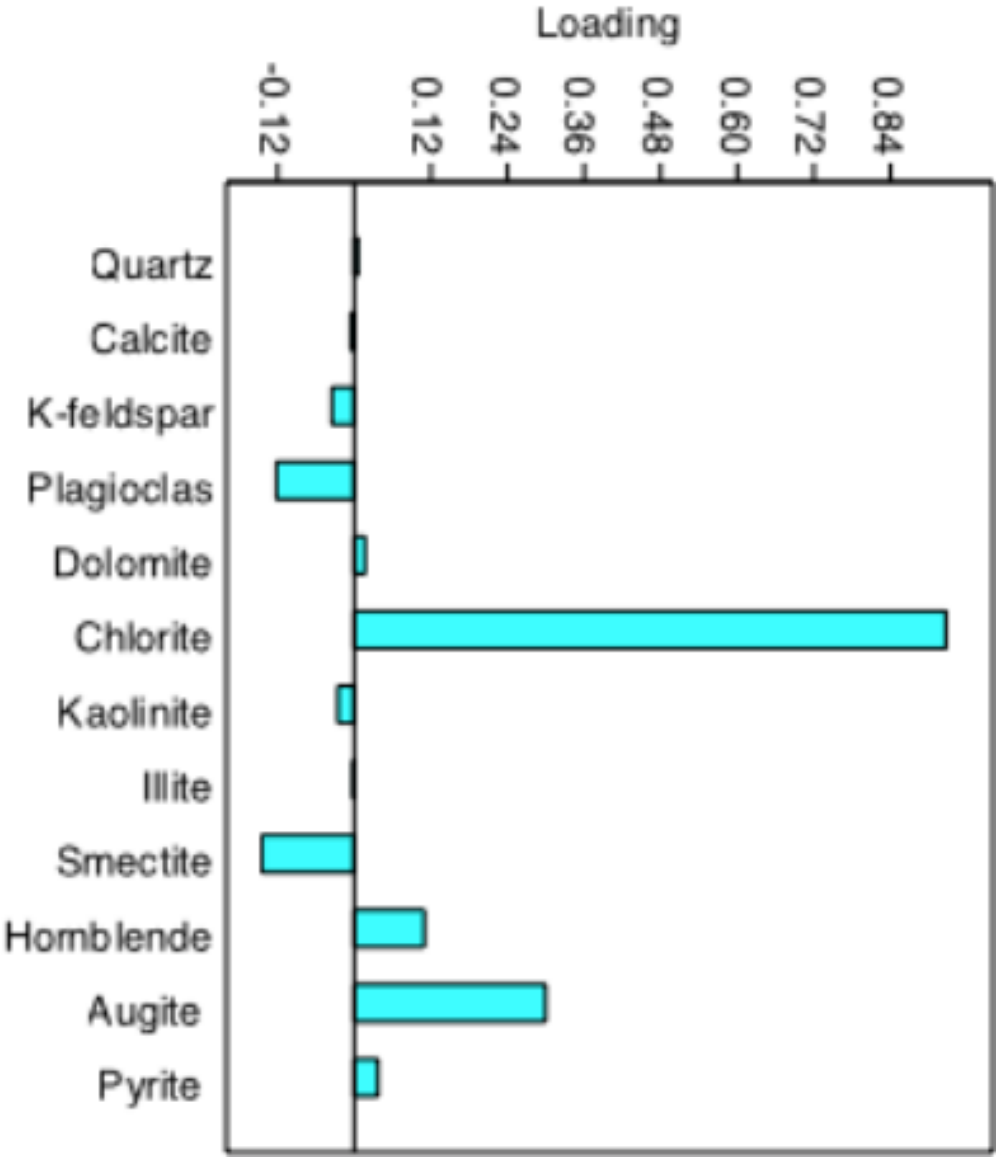

Figure 5: Site U1385 Loading Plot for Principal Component Two

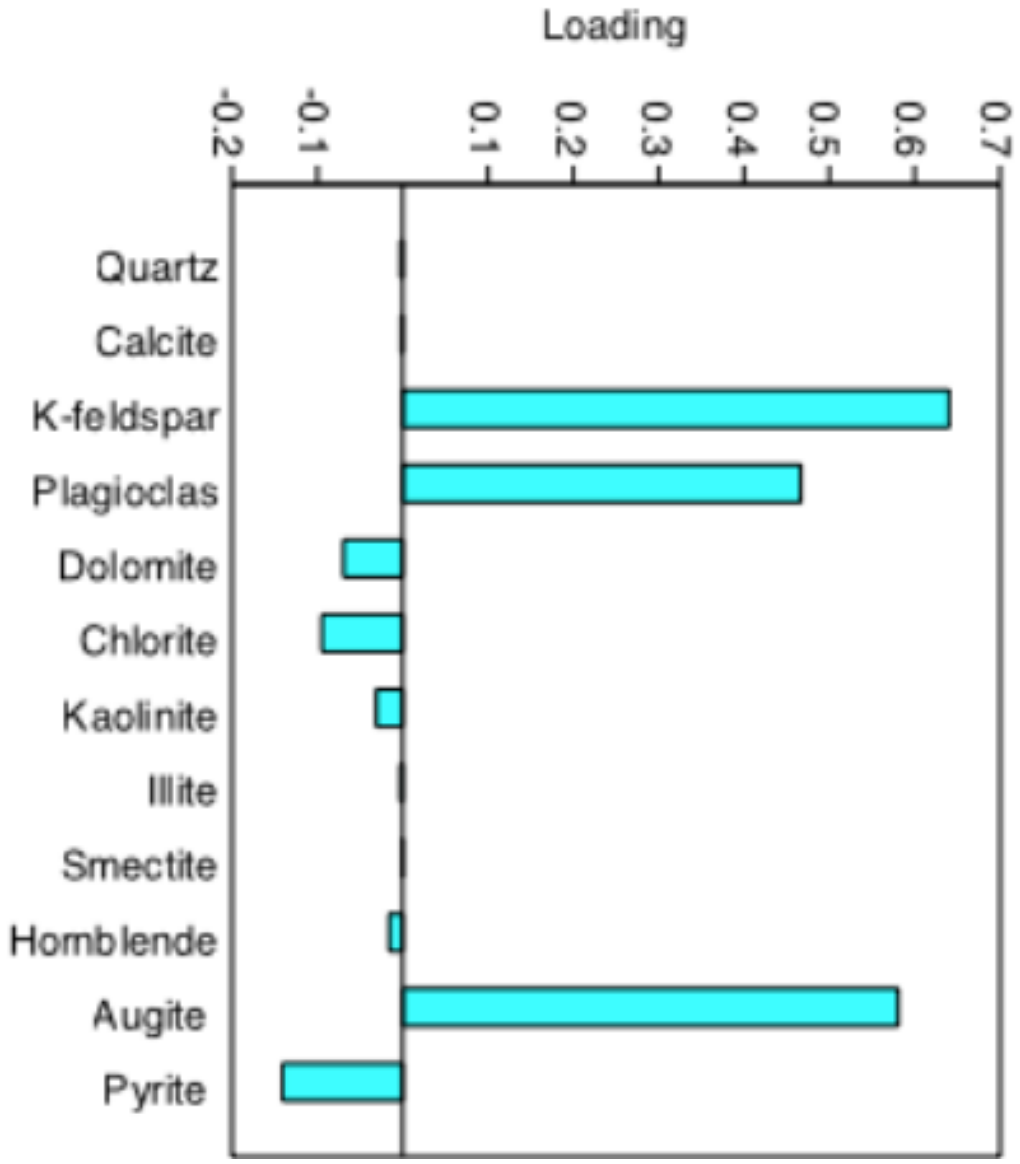

Figure 6: Site U1385 Loading Data for Principal Component Three

Table 2: Loading Data for Site U1385

	PC 1	PC 2	PC 3	PC 4	PC 5	PC 6
Quartz	-2.6E-03	6.1E-03	-2.3E-03	-8.1E-03	-3.7E-03	3.1E-03
Calcite	4.3E-03	-5.4E-03	-1.6E-03	4.5E-03	3.6E-03	-4.8E-03
K-feldspar	-1.7E-01	-3.5E-02	6.4E-01	7.3E-01	8.0E-02	4.8E-04
Plagioclase	7.7E-01	-1.2E-01	4.7E-01	-2.0E-01	-3.2E-01	-3.3E-02
Dolomite	3.6E-01	1.7E-02	-6.9E-02	8.0E-02	5.9E-01	6.5E-01
Chlorite	1.9E-01	9.3E-01	-9.5E-02	1.6E-01	-1.3E-01	2.9E-02
Kaolinite	2.5E-01	-2.6E-02	-3.1E-02	-1.0E-02	6.7E-01	-6.0E-01
Illite	-3.5E-03	-2.3E-03	-2.7E-03	-6.5E-04	9.7E-04	1.3E-03
Smectite	-1.4E-01	-1.4E-01	-5.6E-04	-1.3E-01	-1.9E-03	4.2E-01
Hornblende	-9.0E-02	1.1E-01	-1.6E-02	-8.9E-02	4.3E-02	-2.1E-01
Augite	-3.4E-01	3.0E-01	5.8E-01	-5.6E-01	2.7E-01	8.2E-02
Pyrite	2.8E-02	3.7E-02	-1.4E-01	2.3E-01	5.4E-02	4.9E-02

	PC 7	PC 8	PC 9	PC 10	PC 11	PC 12
Quartz	1.9E-02	4.1E-03	-3.1E-02	-2.3E-01	3.8E-01	9.0E-01
Calcite	-2.9E-03	1.0E-02	2.3E-02	9.7E-01	1.2E-01	2.0E-01
K-feldspar	-4.1E-04	7.6E-02	-9.5E-02	-1.6E-03	7.8E-04	4.0E-03
Plagioclase	1.1E-01	1.0E-01	6.2E-02	-3.6E-03	3.6E-03	-1.9E-03
Dolomite	1.2E-01	-2.2E-01	-1.9E-01	7.1E-03	-2.8E-03	-3.2E-03
Chlorite	-1.3E-01	1.8E-01	-2.9E-02	3.0E-03	-5.2E-04	-3.2E-03
Kaolinite	-1.8E-01	3.0E-01	8.0E-02	-1.4E-02	1.8E-03	6.4E-03
Illite	-2.2E-04	8.4E-03	-1.7E-02	-3.2E-02	9.2E-01	-4.0E-01
Smectite	-8.2E-02	8.7E-01	2.7E-02	-6.4E-03	-9.7E-03	-9.2E-04
Hornblende	8.1E-01	1.8E-01	-4.9E-01	1.9E-02	-1.9E-02	-2.3E-02
Augite	3.8E-02	-1.3E-01	2.2E-01	2.0E-03	5.4E-03	-3.2E-04
Pyrite	5.1E-01	4.3E-02	8.1E-01	-2.2E-02	1.6E-02	5.7E-03

The principal component analysis for Site U1391 defines 13 factors that explain 100% of the original data variance (Table 3). However, only the first three principal components are considered important, based on the distribution of data variance explained by each. These three factors explain approximately 66% of the total data variance (Figures 7-10). Principal Component 1 (Figure 8) accounts for approximately 27% of the variance and is defined by chlorite, which is the only variable with a high positive loading. There is no equivalent high negative loading for Principal Component 1. Principal Component 2 (Figure 5) accounts for approximately 20% of the total variance and is defined by a moderately positive loading for K-feldspar and a high negative loading for plagioclase. Principal Component 3 (Figure 6) accounts for approximately 19% of the total variance and is defined by a high positive loading for augite and a high negative loading for aragonite; this relationship suggests an inverse relationship between augite and aragonite in sediments at Site U1391. Table 4 shows the loading data for all 13 principal components at Site U1391, and Figure 7 shows the SCREE plot, which is a graphical representation of the eigenvalues in the Summary Data (Table 3).

Table 3: Site U1391 Data Summary

PC	Eigenvalue	% Variance
1	2.21E+05	3.81E+01
2	1.36E+05	2.34E+01
3	9.51E+04	1.64E+01
4	4.99E+04	8.60E+00
5	4.03E+04	6.95E+00
6	1.78E+04	3.06E+00
7	1.08E+04	1.86E+00
8	8.57E+03	1.48E+00
9	1.16E+03	2.00E-01
10	3.57E+00	6.15E-04
11	7.86E-01	1.35E-04

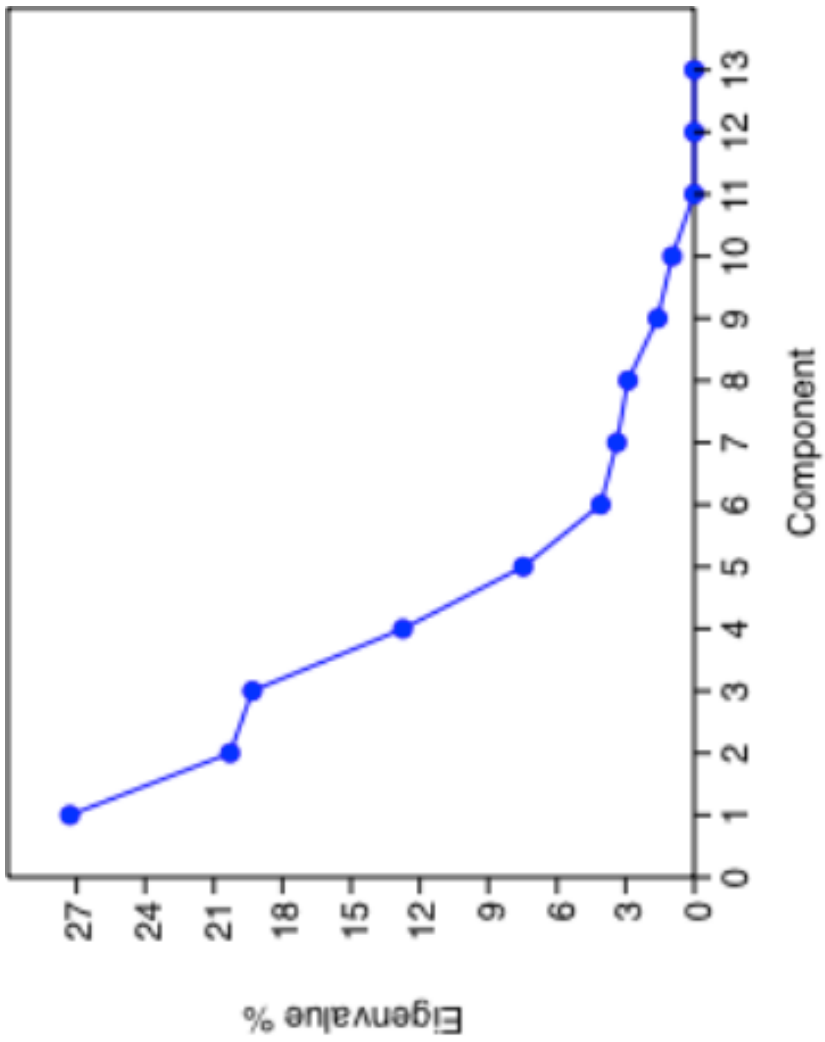

Figure 7: Site U1391 SCREE Plot

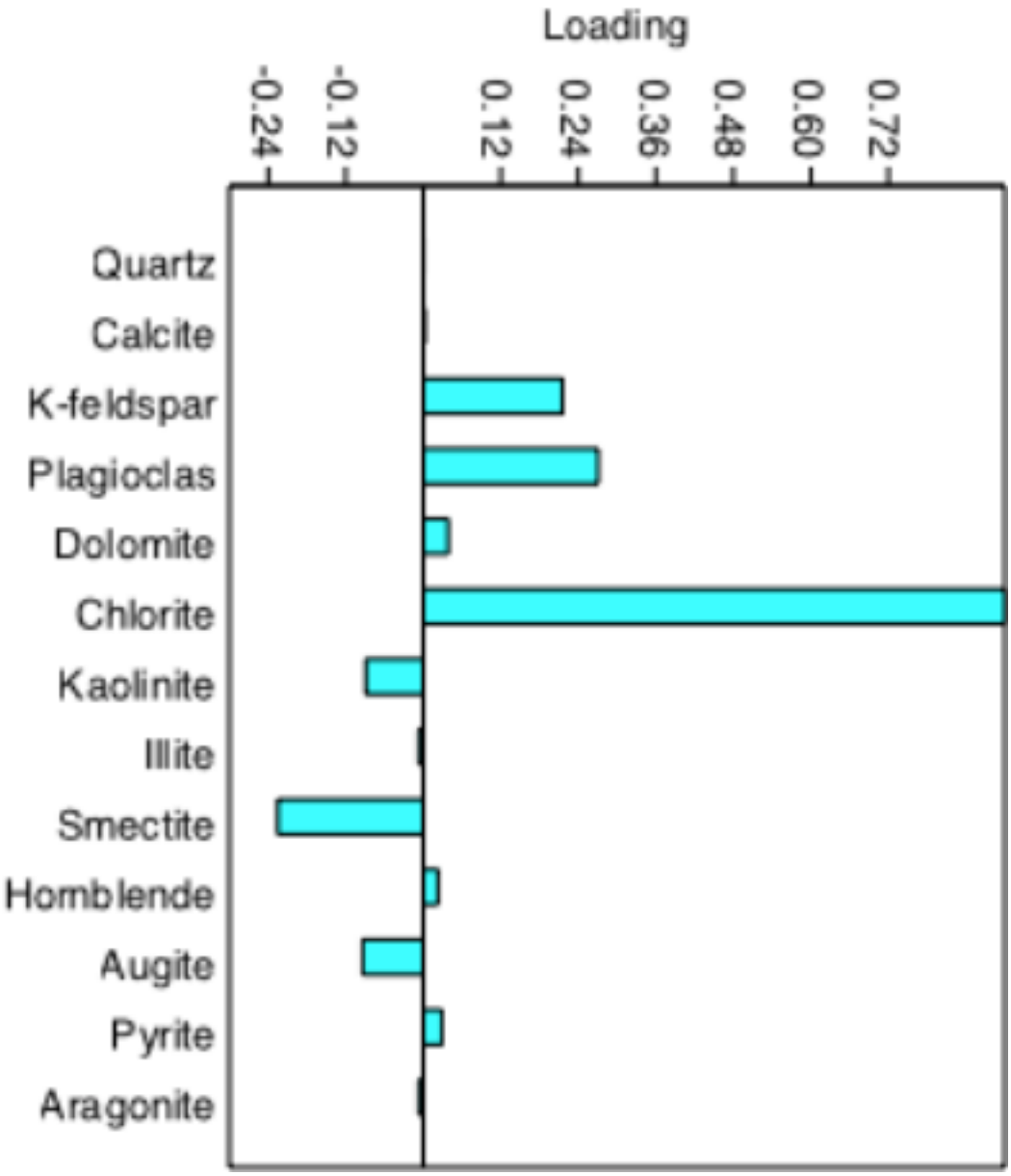

Figure 8: Site U1391 Loading Plot for Principal Component One

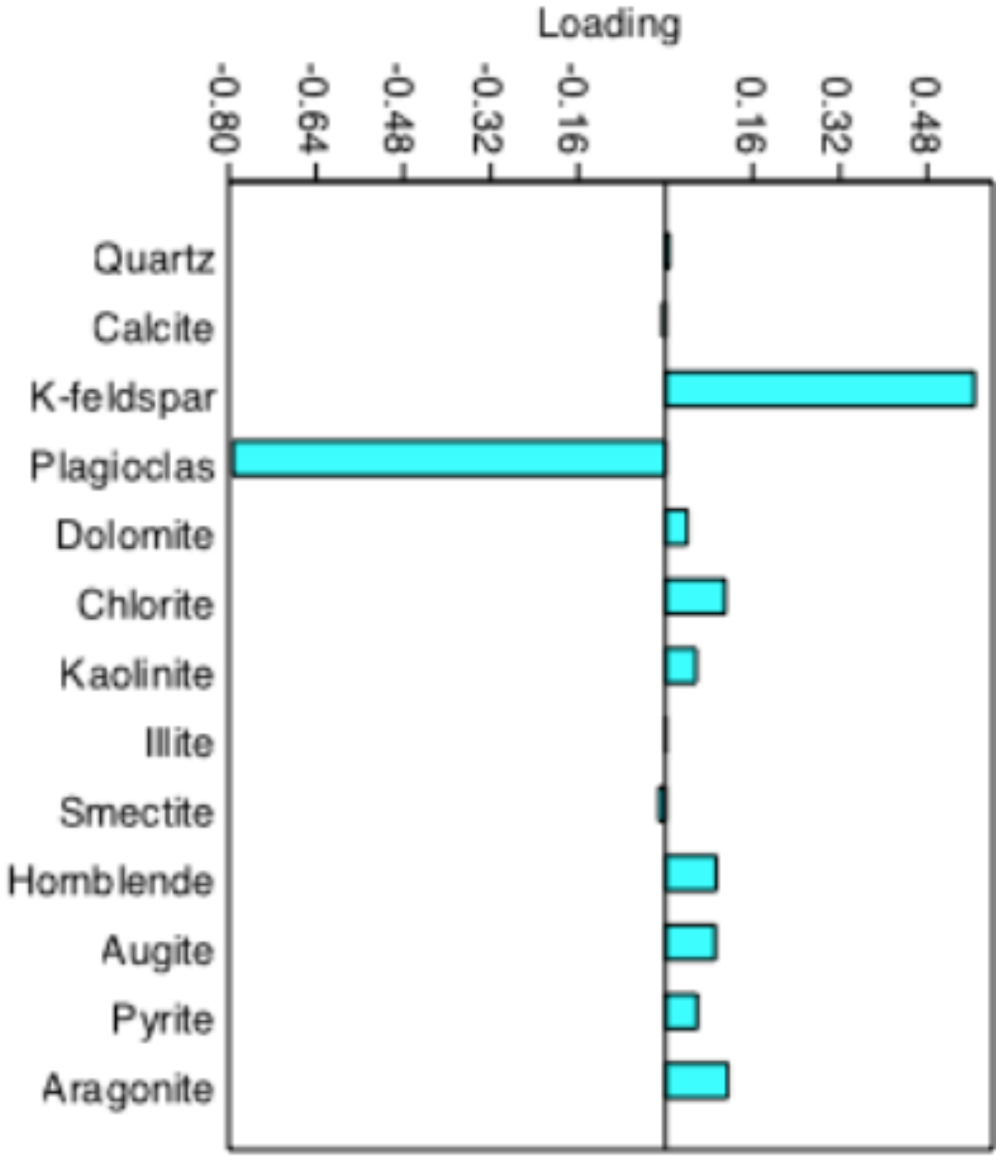

Figure 9: Site U1391 Loading Plot for Principal Component Two

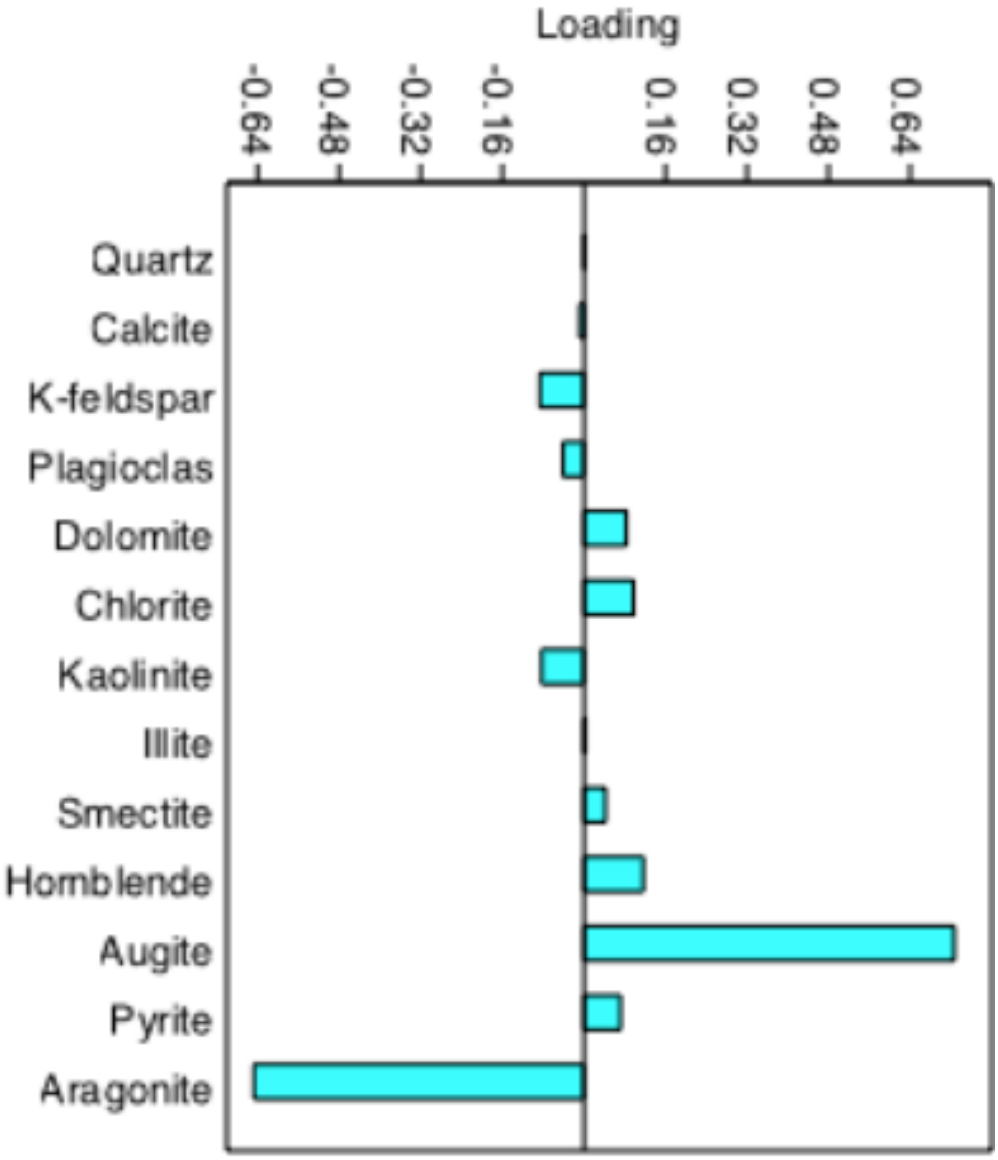

Figure 10: Site U1391 Loading Plot for Principal Component Three

Table 4: Loading Data for Site U1391

	PC 1	PC 2	PC 3	PC 4	PC 5	PC 6
Quartz	-2.6E-03	6.1E-03	-2.3E-03	-8.1E-03	-3.7E-03	3.1E-03
Calcite	4.3E-03	-5.4E-03	-1.6E-03	4.5E-03	3.6E-03	-4.8E-03
K-feldspar	-1.7E-01	-3.5E-02	6.4E-01	7.3E-01	8.0E-02	4.8E-04
Plagioclase	7.7E-01	-1.2E-01	4.7E-01	-2.0E-01	-3.2E-01	-3.3E-02
Dolomite	3.6E-01	1.7E-02	-6.9E-02	8.0E-02	5.9E-01	6.5E-01
Chlorite	1.9E-01	9.3E-01	-9.5E-02	1.6E-01	-1.3E-01	2.9E-02
Kaolinite	2.5E-01	-2.6E-02	-3.1E-02	-1.0E-02	6.7E-01	-6.0E-01
Illite	-3.5E-03	-2.3E-03	-2.7E-03	-6.5E-04	9.7E-04	1.3E-03
Smectite	-1.4E-01	-1.4E-01	-5.6E-04	-1.3E-01	-1.9E-03	4.2E-01
Hornblende	-9.0E-02	1.1E-01	-1.6E-02	-8.9E-02	4.3E-02	-2.1E-01
Augite	-3.4E-01	3.0E-01	5.8E-01	-5.6E-01	2.7E-01	8.2E-02
Pyrite	2.8E-02	3.7E-02	-1.4E-01	2.3E-01	5.4E-02	4.9E-02

	PC 7	PC 8	PC 9	PC 10	PC 11	PC 12
Quartz	1.9E-02	4.1E-03	-3.1E-02	-2.3E-01	3.8E-01	9.0E-01
Calcite	-2.9E-03	1.0E-02	2.3E-02	9.7E-01	1.2E-01	2.0E-01
K-feldspar	-4.1E-04	7.6E-02	-9.5E-02	-1.6E-03	7.8E-04	4.0E-03
Plagioclase	1.1E-01	1.0E-01	6.2E-02	-3.6E-03	3.6E-03	-1.9E-03
Dolomite	1.2E-01	-2.2E-01	-1.9E-01	7.1E-03	-2.8E-03	-3.2E-03
Chlorite	-1.3E-01	1.8E-01	-2.9E-02	3.0E-03	-5.2E-04	-3.2E-03
Kaolinite	-1.8E-01	3.0E-01	8.0E-02	-1.4E-02	1.8E-03	6.4E-03
Illite	-2.2E-04	8.4E-03	-1.7E-02	-3.2E-02	9.2E-01	-4.0E-01
Smectite	-8.2E-02	8.7E-01	2.7E-02	-6.4E-03	-9.7E-03	-9.2E-04
Hornblende	8.1E-01	1.8E-01	-4.9E-01	1.9E-02	-1.9E-02	-2.3E-02
Augite	3.8E-02	-1.3E-01	2.2E-01	2.0E-03	5.4E-03	-3.2E-04
Pyrite	5.1E-01	4.3E-02	8.1E-01	-2.2E-02	1.6E-02	5.7E-03

Discussion

The principal component analysis of mineral abundances at Site U1385 identified three important principal components, and four mineral assemblages, that explain 77% of the data variance. The first principal component, which accounts for 38% of the data variance, is defined primarily by a high positive loading for plagioclase and a moderately negative loading for augite; the difference in the magnitude of these loadings, however, suggests that any inverse relationship between plagioclase and augite is very weak. This high value for plagioclase is interpreted to record a source region of intermediate silicic composition, but also indicates sediments generally coarser than clay size.

Principal Component 2 explains 23% of the data variance, and is only defined by the mineral chlorite. There is no mineral that varies inversely with chlorite. Chlorite is viewed as a mineral formed in terrestrial settings with mafic rocks and little chemical weathering. Therefore, changes in the importance of Principal Component 2 downcore may be indicative of variations in the importance of chemical weathering. In addition, chlorite is a phyllosilicate mineral that becomes more abundant as grain size decreases. For this reason, variations in the abundance of chlorite may be recording differences in grain size of the sediment rather than changes in source area. Given the differences in preferred grain size of plagioclase and chlorite, Principal Components 1 and 2 at Site U1385 may be recording depositionally controlled mineralogical differences.

Principal Component 3 at Site U1385 explains 16% of the data variance, and is defined by a mineral assemblage of K-feldspar, plagioclase and augite. K-feldspar and plagioclase are abundant in a wide range of intermediate composition continental rocks such as siliciclastic, igneous and metamorphic rocks, while augite is found in volcanic material. As a result, Principal Component 3 appears to record the influence of an intermediate volcanic source of sediment.

The principal component analysis of mineral abundances at Site U1391 identified three important principal components, and five mineral assemblages, that explain 66% of the data variance. Principal Component 1 accounts for 27% of the data variance and is defined only by chlorite. As discussed previously for Site U1385, variations in chlorite abundance may record changes in weathering, or changes in depositional energy.

Principal Component 2 accounts for 20% of the data variance and is defined by K-feldspar varying inversely with plagioclase. This difference may suggest variation between a more silicic source of sediment (K-feldspar) and a more intermediate source (plagioclase). Both of these minerals are more common in silts than in clay-sized sediments, so the presence of either is likely to record higher energy conditions of deposition.

Principal Component 3 accounts for 19% of the data variance and is defined by augite that varies inversely with aragonite. Augite is common in volcanic material while aragonite is an unstable polymorph of calcite that most

likely indicates marine biogenic material, such as plankton. As a result, Principal Component 3 appears to record variations between terrigenous and biogenic sediment inputs. Detrital carbonate was also noted in smear slides at these sites, however, so some of this aragonite might also be land-derived carbonate.

Plagioclase, K-feldspar, chlorite and augite are all terrigenous materials while aragonite is a carbonate mineral. These results may distinguish detrital terrigenous vs. marine biogenic sediment, with the terrigenous sediment supplied from the major rivers that empty into the Gulf of Cadiz. Principal Components 1 and 3 at Site U1385 and Principal Component 2 at Site U1391 are all dominated by plagioclase and K-feldspar, which are found in silicic to intermediate composition continental rocks, and in larger grain sizes. Principal Components 2 (Site U1385) and 1 (Site U1391) are dominated by chlorite, which is more common in fine silt or clay-sized sediments.

The variations in chlorite importance may indicate variations in the abundance of fine silt or clay-sized material, deposited during times of weaker currents, when transport and deposition of smaller grains was favored. In contrast, plagioclase and K-feldspar may have been deposited during times of stronger bottom currents, which concentrated the larger grain sizes.

In conclusion, results at both sites may indicate mineralogical variations controlled more by changes in grain size than by changes in local sediment provenance. The original hypothesis was that there would be different

mineralogies at Sites U1385 and U1391 if their sediment sources were different because of the differences in transport paths and processes affecting these two sites (offshore transport +/- wind input at U1385; alongshore transport at U1391). To some extent, this difference can be seen in the differing relationships of plagioclase to K-feldspar at Sites U1385 and U1391. At Site U1385, plagioclase presence/absence alone is indicated by Principal Component 1, and plagioclase variations together with K-feldspar are indicated by Principal Component 3. At Site U1391, however, plagioclase varies inversely with K-feldspar (Principal Component 2). This suggests differences in the sources of plagioclase and K-feldspar for the two sites, even though both sites contain both plagioclase and K-feldspar.

In addition, there is also the possibility that the aragonite is detrital due to the abundant carbonates exposed in the Guadalquivir River drainage, which could be their source. If this aragonite is detrital, then its presence at Site U1391 and absence at Site U1385 is another indication of differences in sediment sources to the two sites. Sources besides the Guadalquivir River also may have supplied sediment to only one of these sites. Sediment supply also may have varied due to differences in wind input and/or erosion along the coastline.

Site U1385 is located farther offshore to analyze open water conditions. Since this site is outside the influence of the MOW, it is expected that its terrigenous sediment may have been transported much farther, and may include wind-derived material. While the sediments at Site U1391 can be

expected to be mud-rich due to its location at the distal end of the CDS, weathering patterns could have varied within drainage basins so that the sediment supplied varied through time. There is also the possibility of changes in strength of the MOW and/or of winds, thereby affecting sediment grain size.

The sediment at Sites U1385 and U1391 could not be tied definitively to distinct source areas, so the mineral assemblages defined by principle component analysis are most directly interpreted as the result of changes in grain size. For these reasons, the Gulf of Cadiz and west Iberian margin are considered a very diverse and complex depositional region, affected by many geological and environmental factors. The mineral composition of its sedimentary records reflects this complexity.

Recommendations for Future Work

In order to further test interpretations of the changes in grain size and sediment provenance, it would be helpful to compare the results of this study to those from related sediment studies of the same region. It would also be wise for one to perform principal component analysis on additional sites near the sites used in this study to better understand the CDS system and MOW in its entirety.

In addition to comparing related studies of the area, it would be beneficial to compare mineralogy of the offshore sediments more directly to the composition of sediments from nearby major rivers such as the Tajo, Guadalquivir and Guadiana that empty into the Gulf of Cadiz and to conduct analyses of the of coastline sediment and Saharan dust composition.

It would also be advantageous to examine downcore data for possible patterns in current strength as interpreted from the abundances of phyllosilicates vs. non-phyllosilicates during glacial vs. interglacial times. By reinserting depth identifiers from the sample data and plotting these results downcore, additional patterns may be identified and interpreted.

References Cited

Expedition 339 Scientists, 2013a. Expedition 339 summary. *In* Stow, D.A.V., Hernández-Molina, F.J., Alvarez Zarikian, C.A., and the Expedition 339 Scientists, *Proc. IODP,* 339: Tokyo (Integrated Ocean Drilling Program Management International Inc.). doi:10.2204/iodp.proc.339.101.2013

Expedition 339 Scientists, 2013b. Methods. In Stow, D.A.V., Hernández-Molina, F.J., Alvarez Zarikian, C.A., and the Expedition 339 Scientists, Proc. IODP, 339: Tokyo(Integrated Ocean Drilling Program Management International, Inc.). doi:10.2204/iodp.proc.339.102.2013

Hernandez-Molina, F., Stow, D. A. V., Alvarez-Zarikian, C., and Expedition IODP 339 Scientists (2013). IODP Expedition 339 in the Gulf of Cadiz and off west Iberia; Decoding the Environmental Significance of the Mediterranean Outflow Water and its Global Influence. *Scientific Drilling, 16,* 1-11. Doi:10.5194/sd-16-1-2013